Rock Mechanics and Rock Engineering (2020) 53:3093–3109
https://doi.org/10.1007/s00603-020-02093-4

ORIGINAL PAPER

Analysis of the Effects of Blasting on Comminution Using Experimental Results and Numerical Modelling

Panagiotis D. Katsabanis[1]

Received: 31 January 2019 / Accepted: 24 March 2020 / Published online: 20 April 2020

Abstract
From blasting to downstream, processes are linked through the continuous reduction of the size of the rock. The effect of blasting is traditionally limited to fragmentation, although effects on crushing and grinding are also recognized and examined in the paper. Fragmentation prediction methods are reviewed to identify issues that need to be addressed in engineering models to improve the accuracy of the predictions. Blastability and energy partition during the blast are key areas for improvement. Damage to the rock, in the form of microcracks, is discussed using experimental findings as well as computer calculations of damage. Experimental results have shown that grindability is affected by energy consumption, which is simplified by the powder factor and by the powder distribution in the blast. Damage calculations show that powder distribution as well as energy partition are important, while the geometry of the blast, borehole pressure, delay time and the complicated stress-wave interaction during the blast play a significant role. To derive a relationship between blasting and milling, analysis of field data, considering lithology, fracture network, detailed blasting parameters and mill performance are needed.

Keywords Blasting · Delay time · Small scale testing · Fragmentation · Grindability · Impact breakage · Numerical modelling

1 Introduction

The importance of blasting to mill operations has been discussed in a series of publications, suggesting that there are two types of benefits of finer blast fragmentation: productivity increase (Grundstrom et al. 2001) and decreased energy requirements at the mill (Michaux and Djordjevic 2005; Workman and Eloranta 2003). While the effects are undeniable, quantification has been less forthcoming. Hence, there are no models allowing engineers to calculate the effects of blasting on mill performance other than the ones relating blasting to size reduction. The latter are often overwhelmed by the influence of powder factor on fragmentation, and often they do not consider important parameters, such as charge distribution, energy partitioning and timing. The purpose of the present paper is to review efforts by the Queen's Explosives Laboratory, analyze them in the context of other findings on the effect of blasting on comminution, and identify issues that need to be resolved to move from the acknowledgement of the effect of blasting on downstream operations to predictive models. The paper is divided in sections on fragmentation, where fragmentation prediction is discsussed, and preconditioning of the rock by blast waves, where the effect of blasting on the grindability of the fragments produced is analyzed.

2 Fragmentation

Blasted ore is further reduced in size by primary crushers, semiautogenous (SAG) and autogenous (AG) mills. SAG mills have special requirements on feed size distribution, which is influenced by the size distribution of the blasted rock (Esen 2013). The 80% passing size, x_{80}, is regularly used to evaluate the energy draw in size reduction (Workman and Eloranta 2003). Hence, predicting the size distribution of blast fragmentation is important. The task is accomplished through models like Kuz–Ram (Cunningham 1983, 1987, 2005), which is based on the estimation of the average size, x_{50}, offered by the Kuznetsov equation, and the Rosin–Rammler or Swebrec equations (Ouchterlony

✉ Panagiotis D. Katsabanis
takis.katsabanis@queensu.ca

[1] The Robert M. Buchan Department of Mining, Queen's University, Kingston, ON K7L 3N6, Canada

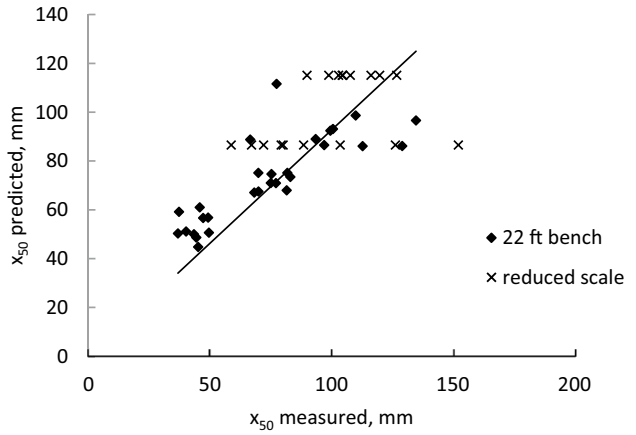

Fig. 1 Measured fragment sizes (Stagg and Rholl 1987) vs. predicted fragment sizes. The prediction was based on the Kuznetsov equation (Cunningham 1983)

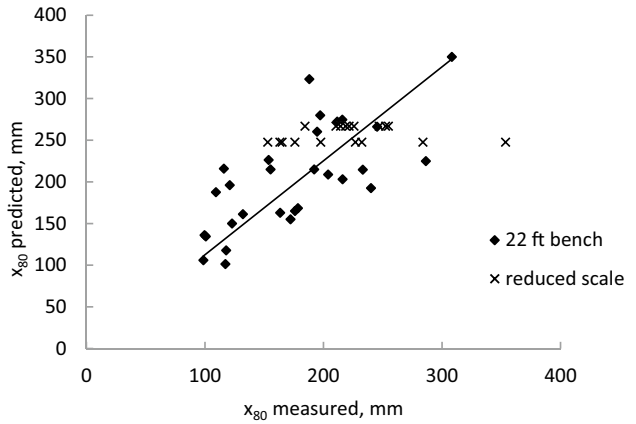

Fig. 2 Measured 80% passing fragment sizes (Stagg and Rholl 1987) vs. predicted 80% fragment sizes. The prediction was based on the Kuz–Ram model (Cunningham 1987)

2005) that need a uniformity index, n, or undulation factor, b, respectively, to shape the fragment size distribution. Often, Cunningham's calculation of the uniformity index is used for either case. Such is the case of the KCO (Kuznetsov, Cunningham, Ouchterlony) model (Ouchterlony 2005).

Unfortunately, the estimation of the average, x_{50}, and the 80% passing, x_{80}, values, based on the above technique, does not appear to be accurate. Figures 1 and 2 show the relationships between measured and calculated x_{50} and x_{80} values in the case of the data set published by Stagg and Rholl, respectively (1987). In the graphs, the prediction of the x_{50} was based on the Kuznetsov equation, with the rock factor A being the average of the values calculated using the Kuznetsov equation and the measured values of x_{50}. The value of x_{80} was calculated using the Rosin–Rammler equation, the calculated x_{50} and the uniformity index equation suggested by Cunningham (2005). For ease of reference, the Kuznetsov and Rosin–Rammler equations, providing the average fragment size, x_{50}, and the fragment size distribution, $P(x)$, are shown in the following equations:

$$x_{50} = AQ_e^{\frac{1}{6}} q^{-0.8} \left(\frac{115}{E}\right)^{\frac{19}{30}}, \tag{1}$$

$$P(x) = 1 - 2^{-\left(\frac{x}{x_{50}}\right)^n}, \tag{2}$$

where A is the rock factor, Q_e the mass of explosive loaded per borehole (kg), q the powder factor (kg of explosive/m^3 of rock), E the relative to ANFO weight strength of explosive (%), and n is the uniformity index.

There are several reasons to explain the discrepancies in the graphs. Kuznetsov's equation, as typically used (Cunningham 2005), calculates x_{50} from the powder factor, the mass of explosive per blasthole and the weight strength of the explosive, while estimating the effect of geology by the rock factor A. It is heavily dependant on the powder factor, and energy partitioning between explosive and rock is not considered. Rather, the total chemical energy of the explosive is considered by virtue of the powder factor and the weight strength. The equation, thus, expresses the intuitive relation between fragmentation and explosive consumption and strength, and utilizes a scale factor by incorporating Q_e to address the issue of explosive (powder) distribution. A correction factor for timing was proposed by Cunningham (2005) based on the early work by Bergmann et al. (1974). The equation considers the blastability of the rock mass by providing an empirical formula for the calculation of factor A, but ignores the often significant variability of the blastability of the rock throughout the blast.

The use of powder factor and lack of energy partition are, in author's opinion, deficiencies in the Kuz–Ram type of engineering models predicting fragmentation. Accurate knowledge of the rock factor is essential, as the factor could be changing even within the same geologic formation, as evidenced from the work of Morin and Ficarazzo (2006). However, in author's opinion, there are more reasons for the discrepancy. Powder factor simplifies explosive performance by the mass of the explosive used. This ignores detonation performance and powder distribution in the blast. The weight strength of the explosive is considered, but the use of the total energy alone cannot describe the ability of an energetic material to create fragmentation. There are many energetic materials with higher energy values than explosives (i.e. some propellants), which would not be able to induce fragmentation since they do not detonate. For detonating explosives, energy partition into shock and heave could be more relevant. Hence, the equation of state of the explosive, in the form of a pressure–volume adiabatic

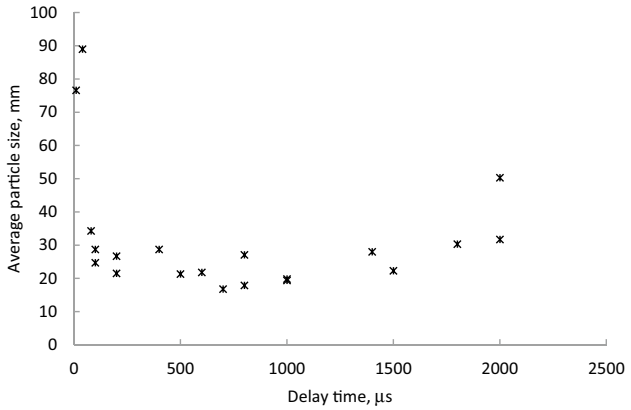

Fig. 3 Experimental observations of the effect of delay time on average fragment size (Katsabanis and Omidi 2015)

relationship, as well as the rock response to dynamic loads are useful in describing the role of explosives on fragmentation. It is also expected that stress waves from various boreholes interact with each other, based on the delay time used. Detailed work by the author in homogeneous small blocks (Katsabanis et al. 2014) and preliminary work by others in small benches (Stagg and Rholl 1987; Otterness et al. 1991) suggest that delay time affects fragmentation. Figure 3 shows the results Katsabanis et al. (2014) obtained using small-scale tests in grout with detonating cord charges. The coarse fragmentation point in Fig. 3, when charges of the same row are detonated instantaneously, is undisputed and observed in various tests (Katsabanis et al. 2006; Johansson and Ouchterlony 2013). With longer delays, the effect of delay time is not as pronounced and was only revealed after several experimental observations. Of interest is the fairly wide range of delays, where very small, if any, changes of the average fragment sizes are observed (Katsabanis et al. 2006; Blair 2010). High speed analysis of the small-scale tests (Katsabanis and Omidi 2015) suggested that the optimum fragmentation occurs well past the time, where the action of stress waves is possible. An undisputed relationship between the fragment size for a given blast and delay time is not available. Cunningham's suggestion (Cunningham 2005) of the existence of an optimum delay time for fragmentation optimization, that depends only on the P-wave velocity of the rock, is a starting point, but oversimplifies the mechanisms of crack propagation.

As mentioned previously, the lack of an accurate description of the rock, the rock factor, is problematic. Cunningham (1987) related this to a blastability index proposed by Lilly (1986). This index is related to the rock mass description, joint spacing and orientation, rock density influence and a hardness factor using an empirical formula and coding suggested by Cunningham (1987, 2005). If one accepts Cunningham's expressions of the blastability parameter A and the fact that rock parameters that control factor A have randomness, one can calculate a variable rock factor A through Monte Carlo simulation. This is shown in Fig. 4, which provides a histogram of values for A in a moderate rock type. This, in turn, creates randomness in the prediction of different sizes of the blast (x_{50}, x_{80}, etc.) and provides a distribution instead of single values (Morin and Ficarazzo 2006).

Recognizing the importance of the rock factor to the prediction of fragmentation, the assessment of blastability has commanded some noteworthy efforts. Latham and Lu (1999) used an energy block transition model, accepting that blasting transforms an in situ block size distribution into a blasted block size distribution. The transformation is related to the blastability of the rock mass. To estimate blastability, Latham and Lu (1999) used Hudson's rock engineering systems (RES) approach (Hudson and Harrison 2000), which is essentially a rock mass classification scheme, in which several parameters affecting blasting were coded in an interaction matrix and subsequently weighted. The approach considers properties of both intact rock and discontinuities and could be used as an alternative to the A factor used in Kuz–Ram. Faramarzi et al. (2013) used the RES approach to calculate a Vulnerability Index, which was later related to the muck pile fragment sizes. The effort showed encouraging results in predicting the 80% passing size compared to the statistical methods and the Kuz–Ram model (Faramarzi et al. 2013).

Alternatively, the use of measurements while drilling (MWD) could provide information on local conditions that could be related to blasting. Katsabanis and Peterson (2011) correlated fragmentation and MWD at a copper–molybdenum open pit mine in a jointed rock mass. The specific drilling energy, in one monitored hole, is shown in

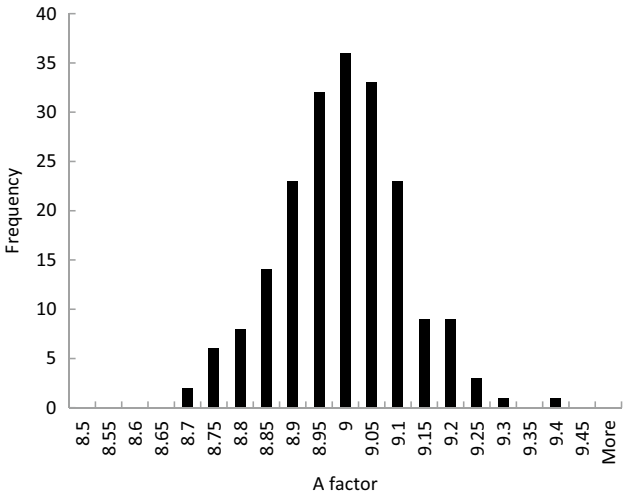

Fig. 4 Blastability value distribution resulting from Monte Carlo simulation of Cunningham's equation (Cunningham 1987) used in Kuz–Ram

Fig. 5 (Katsabanis and Peterson 2011). The trend indicates the change of the rock with depth, while the spikes of the graph indicate sudden changes of drilling parameters (thrust, torque and penetration rate) used for the calculation of the specific energy of drilling. These are probably related to the presence of joints. The MWD information was related to fragmentation around the hole, measured using image analysis at the locations provided by GPS on the digging shovel. Specific energy vs. average fragment size and 80% passing size are shown in Figs. 6 and 7, respectively. Although few measurements were taken in the study, it appears that measurements, while drilling, may be correlated to fragmentation.

The effect of geological structures was not examined explicitly in this work. Obtaining information on the rock structure is challenging and requires monitoring of performance data at small depth increments (Rai et al. 2016). Adebayo and Bello (2014) correlated joint spacing with specific energy of drilling, bit wear rate and uniaxial compressive strength for limestone and gneiss rocks. Khozoughi et al. (2018) compared geophysical logging data with MWD parameters, namely rate of penetration and rotary speed. They determined that MWD parameters could be used to detect open fractures in the case of fractures intersecting a blasthole at near orthogonal angles.

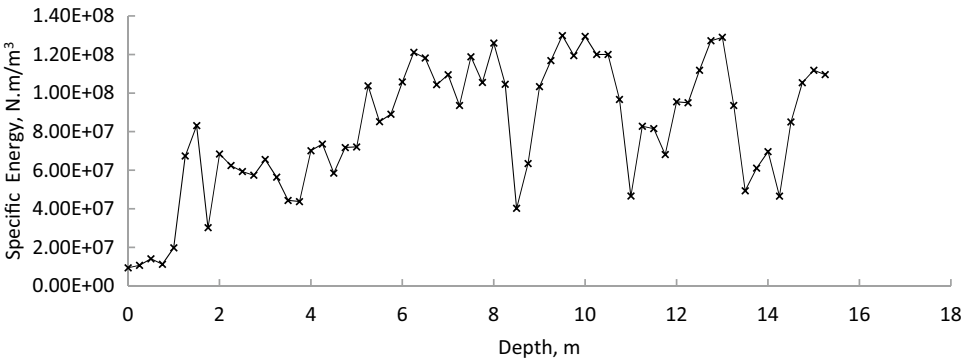

Fig. 5 Specific drilling energy as a function of drilling depth (Katsabanis and Peterson 2011)

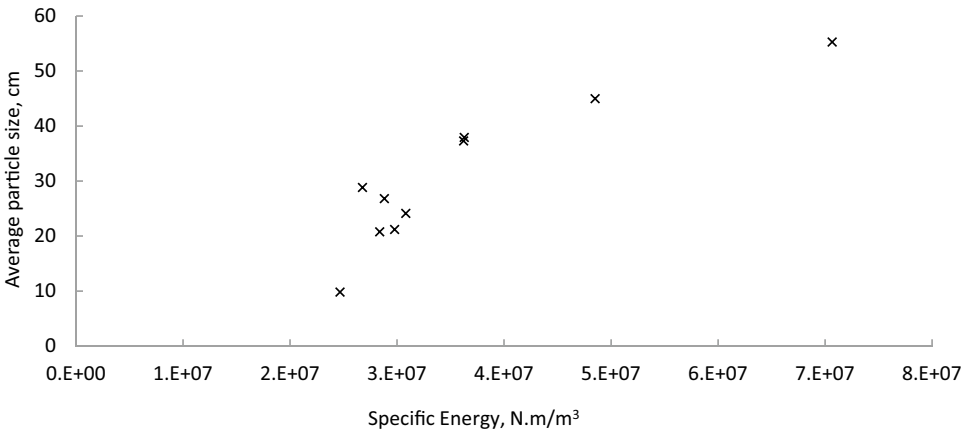

Fig. 6 Measured average fragment size vs. specific drilling energy (Katsabanis and Petersen 2011)

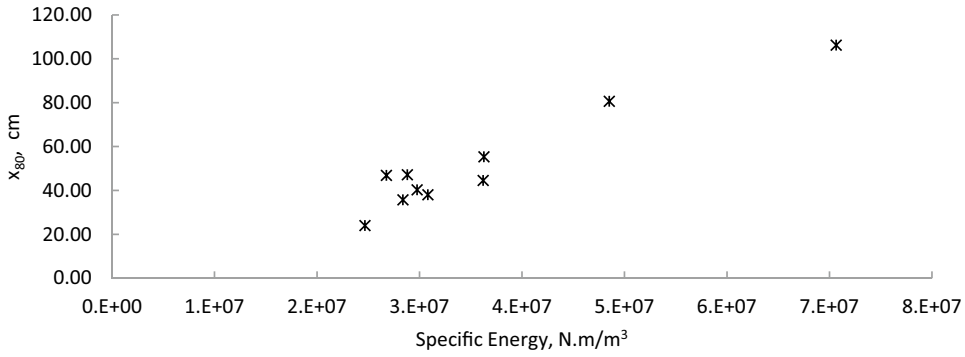

Fig. 7 Measured 80% passing size vs. specific drilling energy (Katsabanis and Petersen 2011)

A further issue in predictive fragmentation models is the estimation of the uniformity index, n, in the Rosin–Rammler function, or the undulation factor b, in the case of Swebrec. Sanchidrian and Ouchterlony (2017) have argued that the Kuznetsov equation is sound and the error lies in the fragmentation distribution. Their analysis of the results from Otterness et al. (1991) suggested that a piecewise Rosin–Rammler with a variable exponent may be appropriate. Hence, their recent model favours the development of prediction equations that do not depend on size distribution functions. In this regard, Sanchidrian and Ouchterlony (2017) have proposed a model adopted from asteroid collision theory and dimensional analysis, where factors for discontinuity spacing and delay time were added. Apart from geometry, rock structure and delay time, the model considers rock strength and explosive energy concentration. According to its developers, the expected error of the model is close to 20% in the 5–100% range of fragmentation.

3 Preconditioning

Nielsen and Kristiansen (1995) presented the effect of blasting on the development of micro cracks, which can be beneficial in the grinding process. The researchers, using blasting in blocks and subsequent grinding of the − 8 to + 2 mm part of the muck, and of the same size material, obtained after crushing the larger fragments of the blast, determined that the former part was significantly easier to grind. This was attributed to micro fractures produced by blasting, which resulted in a reduction of the work index of the material that could amount to an astounding 50% of its original value. Given the inefficiencies of the grinding process, this meant a drastic reduction of the carbon footprint of mining operations and substantial energy savings. This prompted additional work by our laboratory.

3.1 Early Work

3.1.1 Work on Copper Ore Samples

Experiments to examine the effect of blasting on the crushability and grindability of the rock were carried out on a copper–gold porphyry ore from Western Canada. The work was performed by Dan Hikita for his Master's thesis (Hikita 2008). Rock samples from different geological domains were collected at the mining site, and some of the samples were subjected to a blasting effort placing them in an aquarium as shown in Fig. 8 (Hikita 2008). The experiments were conducted inside a blast chamber and all fragments were collected.

To examine the formation of micro cracks, analysis of fracture density was performed in two samples; one subjected to the blast load of the aquarium experiment and the other that was not subjected to any blast load in the laboratory. Thin sections were cut from orthogonal planes and analyzed optically. The fracture densities are provided in Table 1.

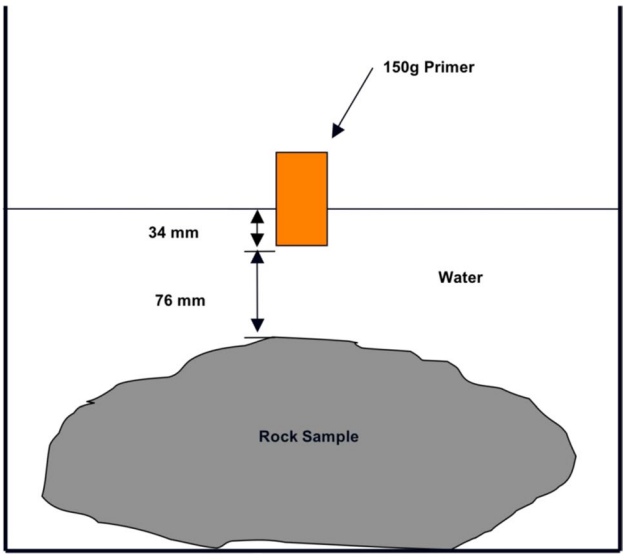

Fig. 8 Schematic of the experiment designed to impact a rock sample by the detonation of a small (150 g) pentolite charge (Hikita 2008)

Table 1 Measured fracture densities before and after blasting (Hikita 2008)

Plane	Fracture density (cm/cm^2) of sample that has not been blasted	Fracture density (cm/cm^2) of sample that has been blasted
Side	1.9	5.0
Front	1.7	7.9
Average	1.8	6.5

It appears that blasting resulted in increased numbers of micro fractures, something that was expected.

Additional tests involved the performance of the Sag Power Index (SPI) test, which is a proprietary test describing the specific power consumption requirements of a material undergoing size reduction in a SAG mill. The test uses a laboratory scale SAG mill, 30.5 cm in diameter by 10.2 cm long, using 2 kg of dry ore crushed to 80% passing of 12.7 mm. Details of the test can be found in Starkey and Dobby (1996).

Table 2 shows the results of the test in samples from different geological alterations of the mine.

Table 2 indicates that domains $D1$ and $D5$ were most likely affected by blasting in the aquarium. In domain $D2$, the effect of blasting cannot be an increase of the SPI index. The result has been affected by sampling, which may have

Table 2 Results of the proprietary SPI test for blasted and not blasted blocks or ore

Geologic alteration	SPI (blasted)/ SPI (not blasted)
D1	1.23
D2	0.95
D5	1.14

also affected the results of *D1* and *D5*. Therefore, only tentative conclusions may be drawn on the basis of few tests.

Additional tests were conducted using a drop-weight test. The drop-weight device consists of a 21.6-kg projectile, made of steel, which falls under gravity on a particle placed on a steel anvil. A cylindrical guide assures vertical orientation of the projectile. The resulting fragments are then screened, and plots of cumulative size distributions are established for different impact energies achieved using different drop heights. The analysis is performed according to Napier-Munn et al. (1996). The point of interest in each of the post- impact fragmentation curves is the fraction of the material passing 1/10 of the initial mean particle size. This is related to the impact energy according to the following formula:

$$t_{10} = A\left(1 - e^{-bE_{cs}}\right), \tag{3}$$

where t_{10} is the fraction passing the 1/10 of the initial size, E_{cs} the specific impact energy (kWh/t), and A and b are breakage parameters calculated from the fit of Eq. (3) to the results of the experiments. Parameter t_{10} indicates how fine the distribution is and a larger t_{10} indicates a finer distribution. In the above formula, A is the limiting value of t_{10} while b is related to the gradient for a constant value of A (Napier-Munn et al. 1996). Typically, variables A and b, on their own, do not carry a significant meaning. However, the product Ab is the initial slope of the t_{10}–impact energy curve, which is indicative of the effect of initial energy input on size reduction. As such, it is considered the best indication of "softening" or decrease of resistance of the rock to impact force during milling. According to Napier-Munn et al. (1996), the product Ab correlates well with performance of SAG mills.

Figure 9 shows the t_{10}–specific impact energy curves for the three different domains of the experiments for both "blasted" and "not blasted" samples.

It appears that the "blasted" samples had higher grindability as demonstrated by the change of the initial slope of the t_{10}–energy curves. Domain $D1$ was affected the most, while the effect on domains $D2$ and $D5$ was marginal.

Bond mill tests were also performed to obtain the work indices of the same samples. The results are shown in Table 3. The results are similar to the previous results on grindability.

The above findings suggested that blasting is likely to be beneficial for grinding. Blasting preconditions the sample, thereby creating microfractures that aid the grinding

Table 3 Work index measurements for different geologic domains alterations (D1, D2, D3) and samples with or without additional blasting impact

Geologic alteration	Work index ("not blasted"), kWh/t	Work index ("blasted"), kWh/t	Change in work index, %
D1	12.7	10.1	20.5
D2	13.0	12	7.6
D5	10.4	10.3	1.0

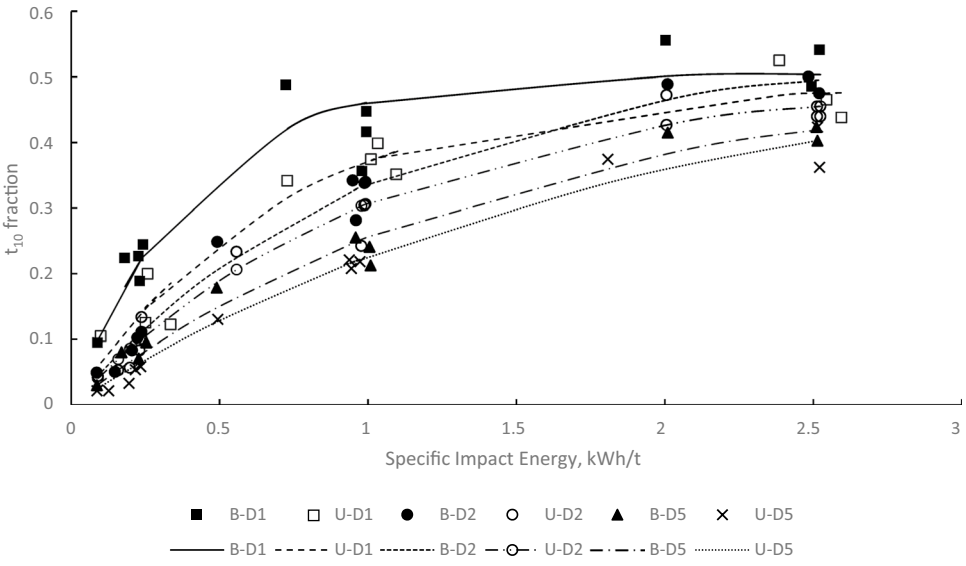

Fig. 9 t_{10} fraction vs. impact energy for different geologic domains (D1, D2, D5). B denotes that the sample was subjected to the impact of a blast produced by a small (150 g) pentolite charge in an aquarium, while *U* indicates that the sample was not subjected to such impact

process. However, the interpretation of the aquarium impact test in the practical blasting effort is not clear. Other issues are the effects of sampling combined with the variability of the rock.

Similar is the experience reported by Kemmeny et al. (2003), who evaluated the effects of blast energy on rock mechanics parameters, crushability and grindability of rock fragments. Their results show that there is a general trend of reduction of strength of fragments with increased blasting energy. However, sampling issues in a production environment resulted in significant scatter.

3.1.2 Measurements of Work Index and P-Wave Velocity in Blocks

A series of experiments were conducted in granodiorite and limestone blocks, which were obtained from dimensional stone quarries to limit variability in the rock, and the effect of blasting effort on damage and the work index of the material were assessed and quantified.

In the case of granodiorite (Katsabanis et al. 2005) the blocks had dimensions of 93 cm × 35 cm × 20.5 cm and the charge consisted of detonating cords placed in 12-mm diameter water-filled holes. The powder factor was kept low (less than 0.18 kg/m^3) to avoid or limit fragmentation of each block to measure P-wave velocities after the blast. Damage was quantified while measuring P-wave velocity before and after the blast. Measurements were taken in consecutive sections 5 cm × 5 cm × 20.5 cm of each block. The average percentage change of the P-wave velocity in each block tested, as a function of powder factor, is shown in Fig. 10.

It appears that the P-wave velocity decreased in every block tested, suggesting that the rock suffered some damage because of the blast. There is a weak trend between the change of P-wave velocity and the powder factor, which may be expected. However, there is a significant scatter of results. More pronounced changes of the P-wave velocity were obtained in the case of cylindrical samples of granodiorite and limestone, which were impacted by detonating cords of various strengths in contact with the samples (Katsabanis et al. 2005). Furthermore, it was observed that in the case of block tests, damage was higher when close to the explosive charges, something that is intuitive, while the average percentage change of the P-wave velocity at each powder factor depended on the delay time used (Katsabanis et al. 2005). Measurements of the point load index, indicative of a change in the crushing resistance of the material, showed a general reduction of the average point load index with the increase of the powder factor, and a decrease with proximity to the charge. An example is provided in Fig. 11 which shows a 35 cm × 35 cm × 20.5 cm block loaded with one strand of 15.9 g/m detonating cord in the centre of the block (powder factor of 0.12 kg of PETN/m^3). The block was divided in smaller blocks of about 5 cm × 5 cm × 10 cm using a diamond saw, which were used in point load testing. Samples were also taken from a piece of granodiorite, which was not subjected to blasting, and were used as a reference.

The grinding resistance of the materials was investigated using the Bond Work Index. In the case of the lower powder factors, where the specimen was not fragmented, the Work Index was determined for the rock close to the borehole, at intermediate distances and at larger distances. This was accomplished by cutting each block in smaller blocks (Fig. 12) and grinding them according to the standard procedure of the Bond mill test.

The results of the Bond mill tests are shown in Table 4 (Kunzel 2003).

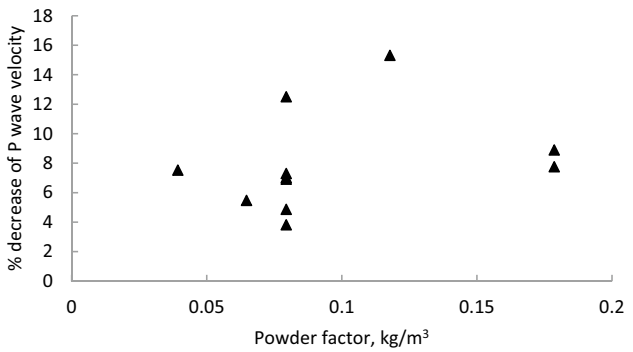

Fig. 10 Average percent change of P-wave velocity vs. powder factor in the experiments of Katsabanis et al. (2005)

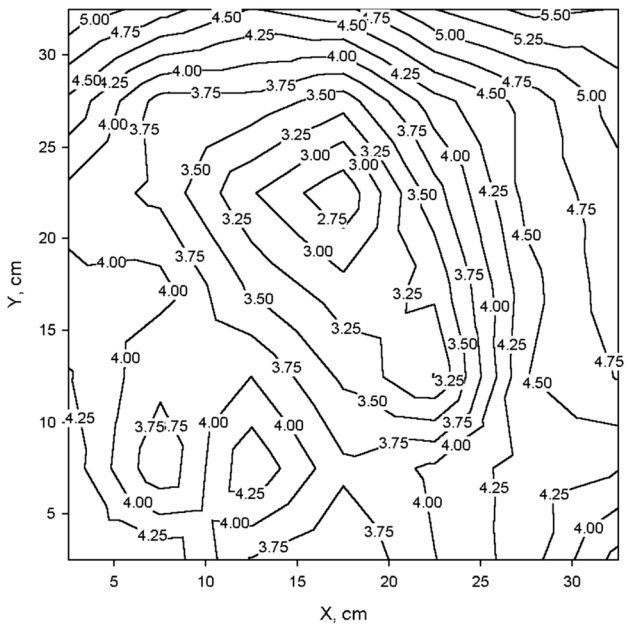

Fig. 11 Point load index in a block detonated by a 10.9 g/m detonating cord. Measurements were conducted on smaller blocks in which the original block was divided (Kunzel 2003)

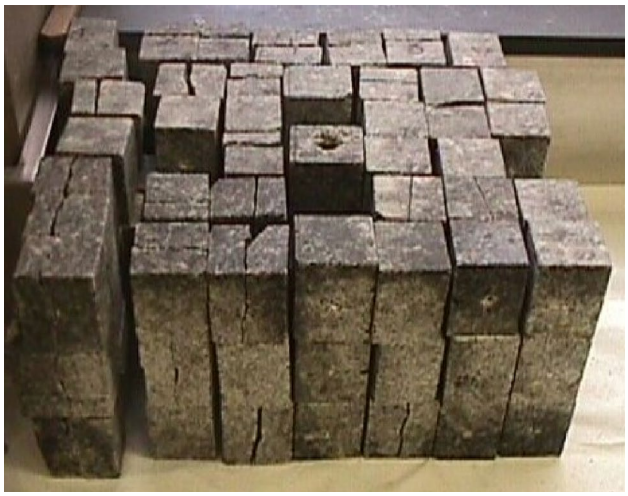

Fig. 12 Division of blasted block in smaller sub blocks (Kunzel 2003)

Table 4 Work index measurements away from borehole in small scale experiments in granodiorite

Sample	W_i (kWh/t)
$q = 0.039\ kg/m^3$	
Inner	13.76
Middle	13.63
Outer	13.53
$q = 0.118\ kg/m^3$	
Inner	12.62
Middle	12.68
Outer	12.67

The work index was reduced as the powder factor increased, but surprisingly, there were no significant changes between the samples at different distances from the blasthole despite the previous findings (P-wave velocity change, point load index and crack density measurement), which had suggested increased damage close to the charge. This could be attributed to two reasons: (a) the accuracy of the Bond mill test and (b) the small powder factor used, which resulted in a small number of cracks and, subsequently, small changes in the sample.

In a subsequent series of experiments, blocks of granodiorite and limestone were blasted using higher powder factors (Katsabanis et al. 2005). The blocks had dimensions 20 cm × 20 cm × 30 cm and were blasted using one borehole with various strength detonating cords. The powder factors used were between 0.24 kg/m^3 and 0.95 kg/m^3 (PETN explosive), and the work attempted to find differences in the work index (a) between two different fragment fractions produced by a blast, assuming that the fraction consisting of the finer fragments originates from the rock closer to the charge, and (b) between different powder factors. The work index was determined using standard rod mill tests and relative ball mill grindability tests (Berry and Bruce 1966). It was found that the rod mill work index of granodiorite decreased by 3% and 8% in the fragments + 11.2 mm and − 11.2 mm, respectively, that were produced by blasting with a powder factor of 0.95 kg/m^3 compared to the sample that was not blasted. Unfortunately, the results of the ball mill tests were not consistent. In the case of granodiorite, no trend could be observed between the work indices of the samples produced by the different powder factors of the experiments and the rock that was not blasted. In the case of limestone, the tests revealed a decrease of the work index of the samples that were blasted vs. samples that were not subjected to the blast. This is shown in Fig. 13.

Relatively smaller changes between the work indices of the samples at different powder factors were observed. The lack of any trend in granodiorite was attributed to the fine grinding that took place in the test, where the 80% product size, after 60 revolutions of the mill, was about 1600 μm, smaller than the average grain size of the material, which was 1670 μm. In the rod mill test, the 80% passing size was around 1900 μm. It appears that benefits of blasting materialize in the coarser stages of comminution in the case of the larger grain material. The inconsistent results prompted the next series of tests (Kim 2010).

3.2 Measurements of Grindability Parameters of Granite Blocks

The experimental work involved blasting of small blocks of different granites; Barre, Laurentian and Stanstead. The rock mechanics characteristics of these granites are shown in Table 5 (Kim 2010).

The blocks of the tests had dimensions 25 cm × 25 cm × 25 cm. The explosive used was typically one, two or three strands of detonating cord, with a linear concentration of 5.3 g/m for each strand, placed inside boreholes having a diameter of 12 mm and a depth of 23 cm. Five

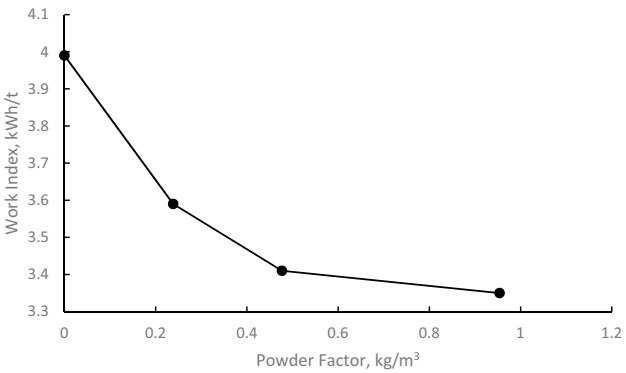

Fig. 13 Work index changes of limestone as a function of powder factor increase

Table 5 Rock mechanics parameters of Barre, Laurentian and Stanstead granites (Kim 2010)

Rock type	Density (g/cm^3)	Elastic velocity (km/s)		Uniaxial compressive Strength (MPa)	Brazilian tensile strength (MPa)	Young's modulus, E (GPa)	Poisson's ratio, ν
		P-wave	S-wave				
Stanstead granite							
XY plane	2.67	3.45	2.21	108 ± 6.8	7.4 ± 0.7	44 ± 3.8	0.20 ± 0.01
XZ plane	2.66	3.70	2.27	115 ± 11.6	7.5 ± 0.5	46 ± 4.9	0.21 ± 0.01
YZ plane	2.67	2.63	1.75	112 ± 8.5	7.6 ± 0.4	39 ± 3.7	0.22 ± 0.02
Laurentian granite							
XY plane	2.65	4.11	2.38	191 ± 21.0	12.3 ± 0.8	65 ± 2.1	0.22 ± 0.02
XZ plane	2.65	4.45	2.77	144 ± 24.8	11.5 ± 1.0	59 ± 3.0	0.21 ± 0.01
YZ plane	2.65	4.51	2.82	174 ± 20.2	12.6 ± 1.1	72 ± 5.6	0.22 ± 0.01
Barre granite							
XY plane	2.63	4.32	2.28	137 ± 10.0	12.0 ± 0.8	53 ± 5.5	0.22 ± 0.03
XZ plane	2.64	3.91	2.25	137 ± 12.7	11.0 ± 1.2	52 ± 0.4	0.21 ± 0.01
YZ plane	2.64	4.19	2.40	130 ± 11.0	10.5 ± 1.0	54 ± 2.4	0.24 ± 0.03

boreholes were drilled using a dice pattern with four boreholes drilled at the corners of a 12.5 cm × 12.5 cm square and the fifth hole placed at the centre of the square. The coupling medium was water. In some experiments, the explosive was waxed RDX, which was fully coupled to the borehole and its mass was adjusted to provide the same energy as the PETN of the detonating cords. Coupling the explosive fully to the borehole definitely changes the peak pressure that is transmitted to the rock as well as the characteristics of the pressure pulse. However, the purpose of the experiments was to investigate the role of the powder factor, charge distribution and timing on fragmentation and grindability. After each test, the fragments were collected, screened and subjected to the drop weight test as described earlier. The grindability parameters A and b were determined from the analysis of the t_{10}–impact energy relationship. The results of the tests, where only the powder factor varied, are presented in Fig. 14. It appears that Stanstead granite exhibited the

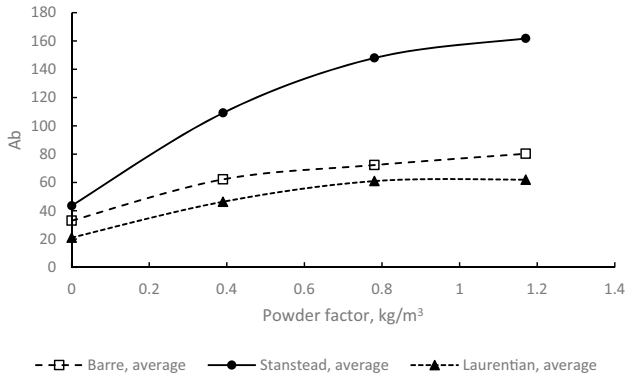

Fig. 14 Grindability parameters (*Ab*) of three types of granite vs. powder factor used in the experiments

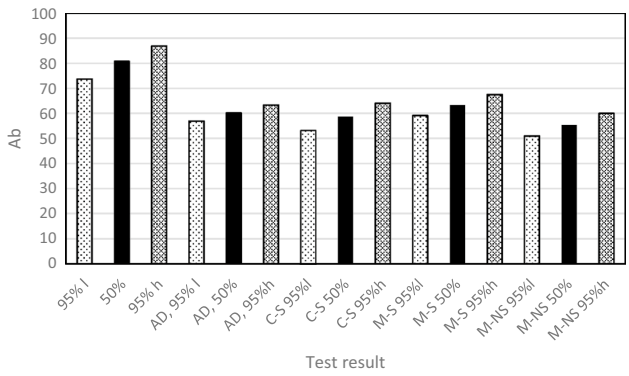

Fig. 15 Grindability parameter (*Ab*) values (95% lower, average and 95% higher) of Barre granite for various charge distributions and the same powder factor

highest effect, while the other two rocks showed diminishing improvements of grindability as the powder factor increased.

The effect of charge distribution was also examined in some blocks of Barre granite using pressed *RDX*, placed in one central borehole with a diameter of 12 mm. The powder factor was kept to 1.17 kg/m^3 of PETN and the results are shown in Fig. 15, where the average as well as the 95% lower and upper values of the *Ab* grindability parameters is provided and indicated by the leter *l* and *h*, respectively. In the figure, *AD*, *C*, and *M* indicate air deck, concentrated charge at the bottom and concentrated charge in the middle, respectively, and *S, NS* indicate the presence or absence of stemming, respectively. Thus, the label *C–S 95% l* indicate the case of a concentrated charge at the bottom of the hole with stemming and the value represents the lower 95% confidence level. Clearly the results of the tests, where the charge is concentrated, are inferior, suggesting that charge distribution is important.

3.3 Analysis of Grindability and Damage

Numerical modelling of the experiments was performed using ANSYS AUTODYN (AUTODYN 2009), a finite element code used to model material response to stress and shock waves. It is a continuum model, which means that the rock, at all times, is treated as a continuum and gases are not allowed to penetrate cracks formed due to stress wave propagation. Cracks here are simulated by failed elements. What is modelled is the evolution of damage due to stress waves and subsequent strength reduction due to damage. To model damage due to blasting and the effect of charge distribution in a blast, the RHT damage model for concrete (Riedel 2009) was used. While there are several other models predicting damage in blasting, the RHT model was selected since it is readily available in commonly used codes (AUTODYN, LS-DYNA) and has been used successfully to model blast damage (Xie et al. 2017; Yi et al. 2012). Damage in the model is expressed by a factor *D*, defined as (Brannon and Leelavanichkul 2009)

$$D = \sum \frac{\Delta \varepsilon^p}{\varepsilon^f}, \tag{4}$$

where Δ^p is the plastic strain and ^{f} is the failure strain given in the following equation:

$$\varepsilon^f = D_1 \left(\frac{p}{f_c} - \frac{p_{\text{spall}}}{f_c} \right)^{D_2}, \tag{5}$$

where D_1 and D_2 are user specified constants having values of 0.04 and 1, respectively, in the present calculations (default parameters), p the pressure, p_{spall} the spall strength, and f_c is the compressive strength of the material.

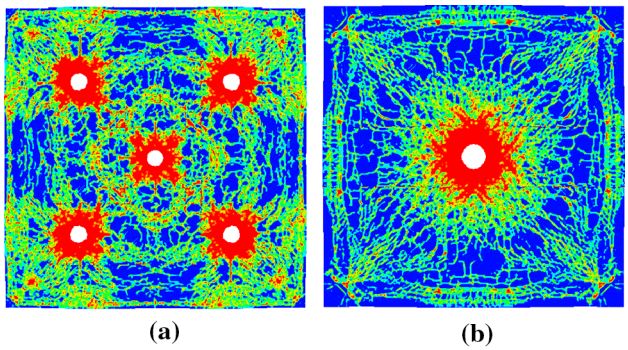

Fig. 16 Calculated damage (**a**) for explosive distributed in five holes and (**b**) the same explosive mass concentrated in a single hole

Table 6 Basic rock mechanics parameters for rock used in numerical modelling calculations

Porous density	2.72 g/cm^3
Solid density	2.75 g/cm^3
Porous sound speed	3542 m/s
Bulk modulus	35.27 GPa
UCS	140 MPa
Shear modulus	20.60 GPa
Compressive Strength	140 MPa
Shear strength	39 MPa

The value of *D* is between 0 and 1 and allows the calculation of the reduction of the strength of the material, interpolating between the limit and residual yield surfaces of the material. Calculations of damage were mostly done in a planar geometry; the pulse from the explosive charge was obtained from an axisymmetric simulation, where the length of the charge, coupling and the point of initiation were considered. The pulse was then used as a dynamic boundary around the circumference of the boreholes of the planar model. The density of the explosive was 1.26 g/cm^3 and the JWL parameters provided by Dobratz and Crawford (1985) were used. Figure 16 compares the damage with a level above 0.4, representing both visible fractures and microcracks, when the charge was distributed in 5 holes versus when the charge was concentrated in one blasthole. The element size is 1 mm × 1 mm, permitting localization of damage. Thus, it can show crack propagation as well as areas where the strength of the rock is reduced due to the development of micro cracks, which may be related to grindability. The threshold of damage of 0.4 was selected arbitrarily, assuming that the effect of stress waves at a level below this is not significant. The main rock mechanics parameters, used for the calculation of the damage contours, are given in Table 6, and they are very close to the parameters in the AUTODYN library for concrete with a strength of 140 MPa (AUTODYN 2009). Despite the fact that the model has not

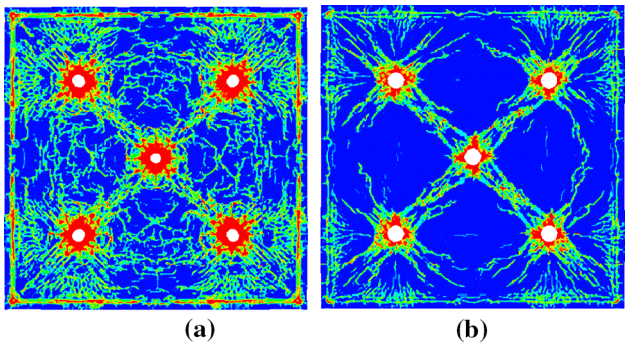

Fig. 17 Calculated damage levels for air decoupled charges (**a**) and low-density charges coupling the holes and maintaining the same powder factor (**b**)

been calibrated, the trends can be considered reliable since the same parameters were used in both runs. The calculations show that significantly less damage resulted when a concentrated charge was used, similar to the experimental results. The model was used to test the effect of other parameters which were not examined experimentally. Figure 17 shows the damage contours in the case of air as a coupling medium, and when low-density PETN fills the drilled hole so as to maintain the powder factor of the experiment. The density of the PETN in this case was 0.132 g/cm^3. The performance parameters for the low-density PETN were calculated using the Cheetah code (Fried 1996), and the JWL parameters required in the numerical model were obtained from the fit of the calculated isentrope passing through the detonation state. These are given in Table 7.

The calculated damage contours are significantly different than in the case of the water-coupled calculations. Clearly, air decoupling reduces damage and the low-density explosive creates much less damage, despite the powder factor being the same. Hence, explosive performance, and not just total energy yield, is important. Apparently, the use of powder factor oversimplifies the complex interaction between the stress wave provided by the explosive and the rock.

Katsabanis and Kim (2011) were able to use all the data collected from the drop-weight tests to describe the relationship between the fraction t_i, passing $1/i$ of the initial size of the fragment subjected to a drop-weight energy of E as well as the powder factor q that was used in the blast. They proposed the following expression:

$$t_i = A_i\left(1 - \mathrm{e}^{-b_i(1+c_i q)E}\right), \tag{6}$$

where A_i, b_i and c_i are constants, q the powder factor, and E is the energy of impact. The use of the powder factor is justified here as all other parameters were kept constant.

The derivative of Eq. (6) with respect to the energy of impact is

$$\frac{\mathrm{d}t_i}{\mathrm{d}E} = A_i b_i\left(1 - \mathrm{e}^{-b_i(1+c_i q)E}\right)\left(c_i q + 1\right), \tag{7}$$

which can easily provide the initial slope of the t_i–E curve that has been traditionally related to softening of the rock mass.

This, however, suggests that the initial slope of the size–energy relationship is linearly related to the powder factor. However, there is evidence that the relationship is parabolic as indicated in Fig. 14. Hence, an improvement of the relationship would be

$$t_i = A_i\left(1 - \mathrm{e}^{-b_i(1+d_i q^{0.5})E}\right), \tag{8}$$

where d_i is a positive number from the fit of experimental data. The initial slope of the t_{10}–E relationship has the following form:

$$Ab = Ab_0\left(1 + d\sqrt{q}\right), \tag{9}$$

where Ab is the initial slope of the t_{10}–impact energy relationship at powder factor q and Ab_0 is the initial slope of the curve for the material prior to blasting. The values of Ab_0 and d for the various materials of the tests are shown in Table 8.

Napier-Munn et al. (1996) has suggested the following relationship for Ab as a function of the Work Index of the material:

$$Ab = 117 - 3.5WI \tag{10}$$

Examining the original data, provided by Napier-Munn et al. (1996), it can be observed that the coefficient of determination of the fit is very poor. Napier-Munn et al. (1996) warned that the correlation should not be expected to be strong as the work index in the mill measures the reaction of the feed to a combination of impact and abrasion (Napier-Munn et al. 1996), while Ab is based entirely on impact. Limited

Table 8 Ab_0 and d values used in Eq. (9) for the three granites

	Ab_0	d
Barre	33.5	1.31
Stanstead	43.2	2.57
Laurentian	21.6	1.86

Table 7 Calculated JWL parameters for PETN at a density of 0.132 g/cm^3

A (GPa)	B (GPa)	C (GPa)	R_1	R_2	ω	E_0 (kJ/m^3)
70.7157	3.0852	0.1763	27.5554	8.9253	0.3273	5.5×10^5

observations of Katsabanis and Kim (2011) have suggested different relationships between the grindability parameters, *Ab*, and the work index, *WI*, due to the increase of the powder factor in blasting, as follows:

Laurentian granite:

$$Ab = 792 - 62WI \tag{11}$$

Barre granite:

$$Ab = 516 - 42WI \tag{12}$$

Stanstead granite:

$$Ab = 1180 - 90WI \tag{13}$$

Considering Eqs. (9), (11), (12) and (13), the tentative effect of the powder factor on the work index is shown in Fig. 18 for the case of the three granites. It appears that a substantial change in powder factor may be required for a significant change of the work index.

According to the previous figures of the damage calculations, damage is not uniformly dispersed in a blast. The zone around the explosive may be considered fully damaged, containing macro and microcracks, while, as distance increases, damage levels drop. Damage is also affected by the geometry of the blast. Figure 19 shows the distribution of damage around a single 160-mm diameter, 12-m long borehole loaded with ANFO, with a density of 0.93 g/cm^3 and a collar of 3.3 m. The modelling is axisymmetric and the only free boundary is the top one, representing the surface of the ground. The rest of the boundaries are non-reflective which means that the charge is confined. The calculation was performed using the AUTODYN code with the *RHT* model and the same material properties as in the previous calculations. The JWL equation parameters obtained by Davis and Hill (2002) were used to model ANFO.

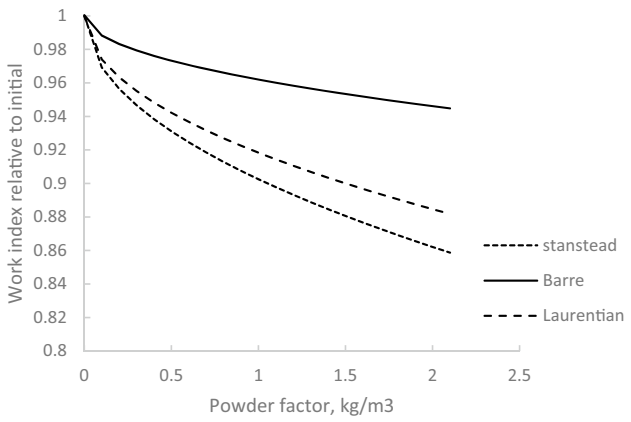

Fig. 18 Work index relative to not blasted material vs. powder factor for three granites

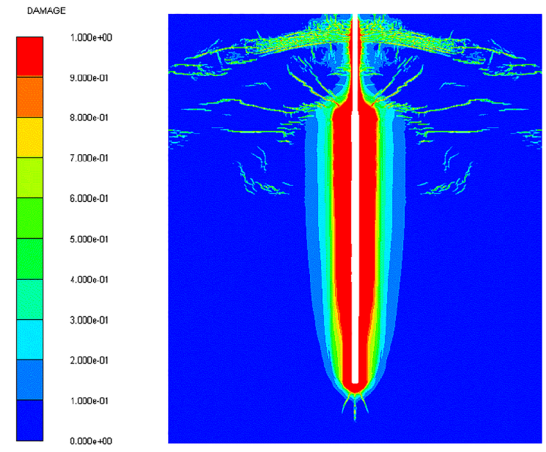

Fig. 19 Damage distribution around a 160 mm diameter borehole in an axisymmetric calculation using AUTODYN

The calculations here show that extensive damage extends a distance of approximately 1.2 m in radius, while individual cracks may run longer distances, especially when free boundaries will most likely be present in the blast. The collar has sustained little damage, indicating a zone where fragmentation will be poor, and the effect of blasting on crushing and grinding will be small. The figure reinforces the previous conclusion that a significant increase of powder factors is required for grindability improvements. However, a blast contains many holes, which, apart from distributing the explosives in the rock to be blasted, result in interactions between the stress waves produced when the charges detonate. Thus, the blasting pattern as well as the time delay between boreholes should play a role in damage development. Katsabanis and Omidi (2015) have shown the effect of delay on fragmentation in small-scale blasts. It is not certain

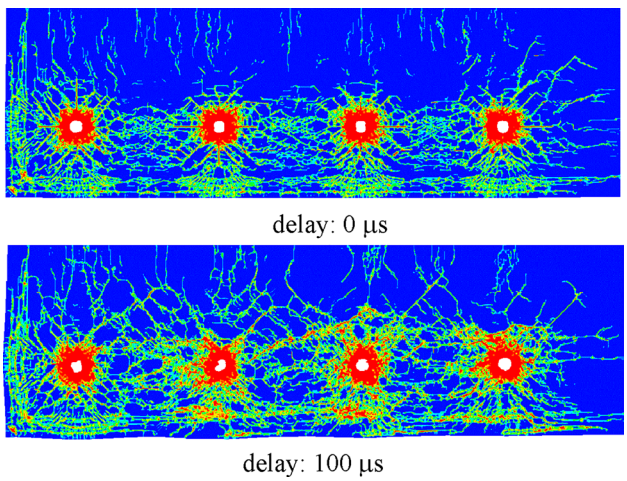

Fig. 20 Calculated damage for delays of 0 µs and 100 µs between holes in a small scale blast (burden = 7.5 cm)

that microfracture development follows the same relationship, as macrocracks may appear late in the process due to the action of the gases of the detonation. The AUTODYN code was again used to model small-scale experiments, similar to the ones conducted in the field. The element size in the model was 1 mm × 1 mm. The experimental set up was such that the burden was 7.5 cm, the spacing 15 cm and the borehole length 23 cm. The borehole was loaded with detonating cord with a linear charge concentration of 21.3 g/m and the coupling medium was water. Figure 20 shows the resulting damage from modelling in planar geometry and using delays of 0 μs and 100 μs between holes.

There are similarities and differences between the calculation and the experiment. In the case of the 0 μs delay, damage is concentrated between the holes and there is less back break, similar to the experiment. Although the damage is different between the two cases, it is not certain that the damage is less in the case of instantaneous initiation. Fragmentation was clearly coarser in the experiment with instantaneous initiation (Katsabanis and Omidi 2015). However, if one increases the burden, the situation appears to be different. Figure 21 repeats the damage contours of delays 0 μs and 100 μs, respectively, but with an increased burden of 15 cm, instead of 7.5 cm.

Damage in this case resembles what was obtained in the experiments of Omidi (Katsabanis and Omidi 2015). The reflected wave from the free face is of importance here. If damage between holes is established prior to the reflected wave reaching the line of the row of the boreholes, it creates a barrier for further propagation of damage. This happens if the burden is sufficiently long or the spacing is sufficiently short. Otherwise, the cracks between holes do not have time to join, and cracks beyond the line of the row are formed. This has been determined experimentally in the work of Olsson et al. (2002). Hence, distances between boreholes, sequencing and delays appear to play a role on damage development. To investigate this, blast patterns of small-diameter boreholes were modelled using AUTODYN. Hole diameter, explosive loading and rock were the same as before.

Figure 22 shows cracked elements with a square pattern and a staggered pattern, respectively, at different delay times. The free face is at the bottom of each graph. The difference in the damage patterns is, however, clear and possibly unexpected. While it is expected that the staggered

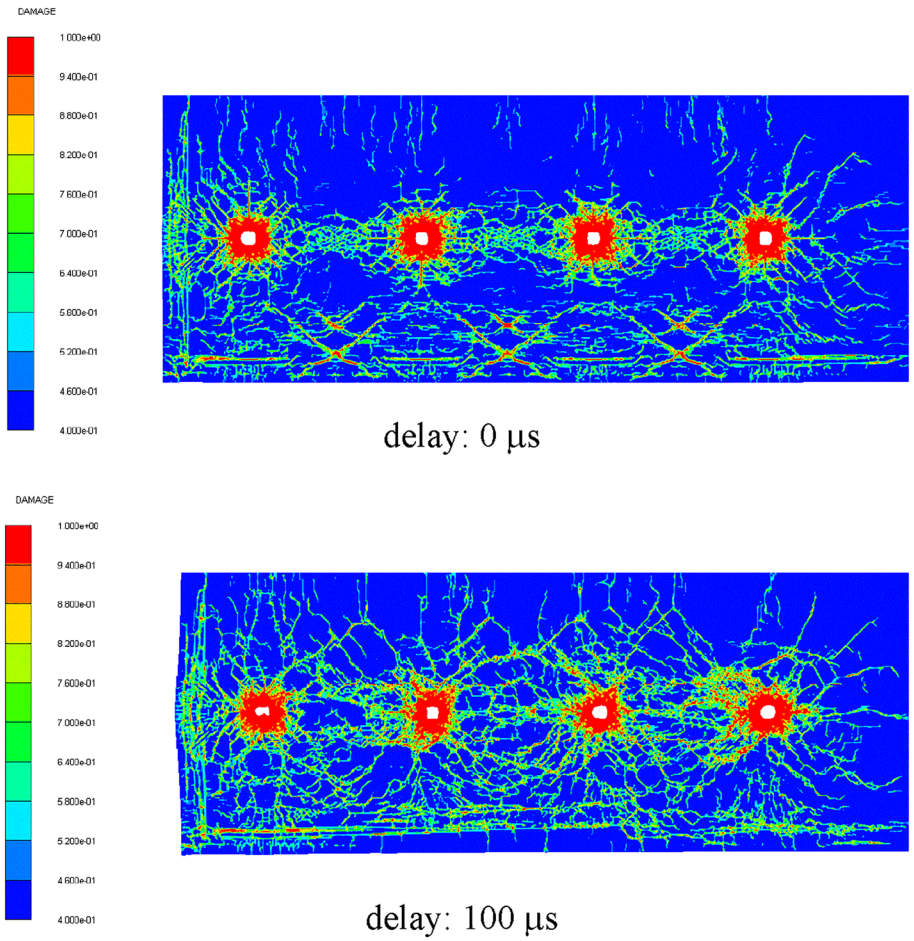

Fig. 21 Calculated damage for 0 μs and 100 μs delays between holes in small scale blasts with burden equal to spacing (burden = 15 cm)

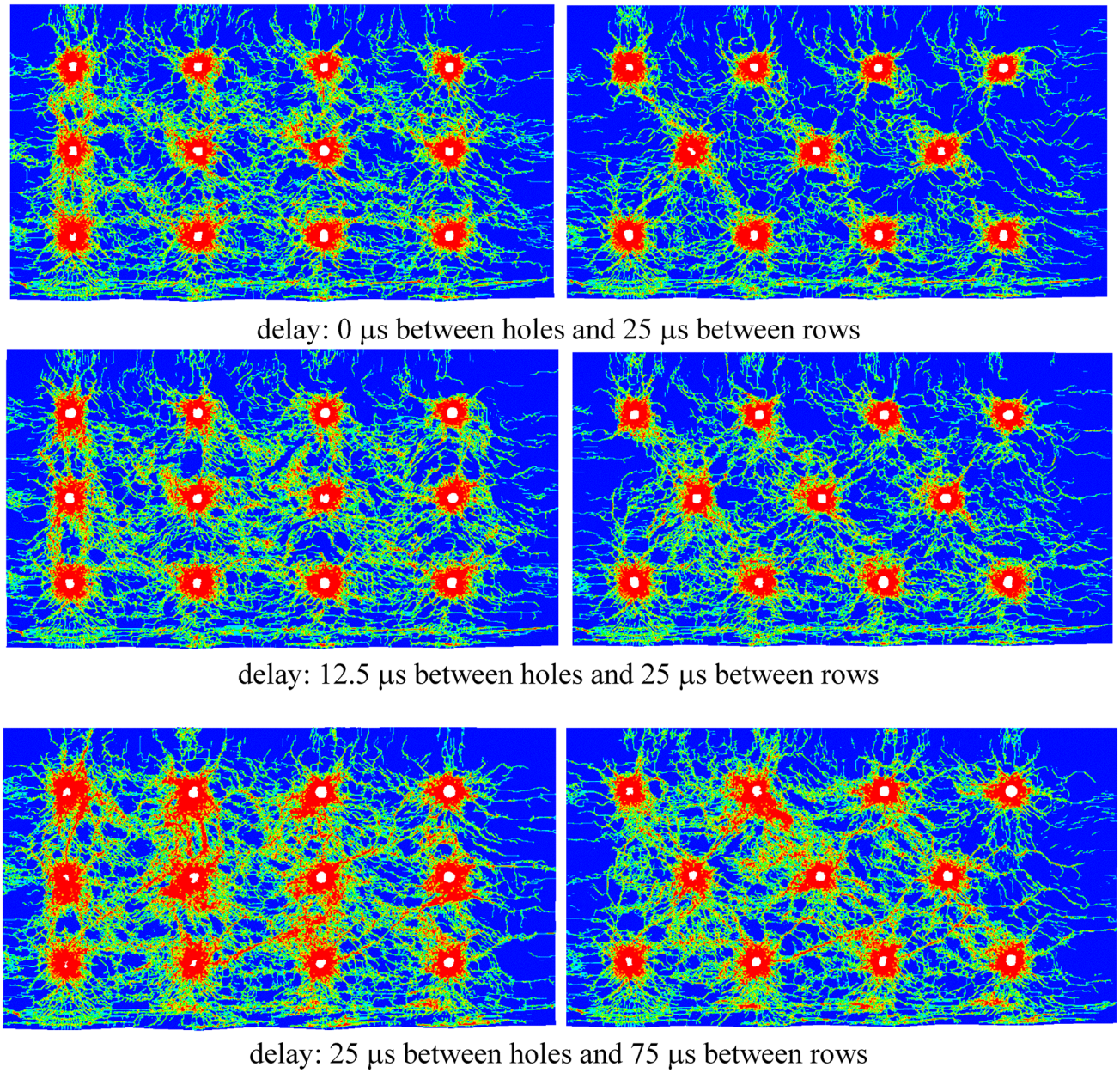

Fig. 22 Calculated damage in multi row small scale blast with different delays and different patterns. The burden for all cases was equal to 7.5 cm

pattern offers a better distribution of powder, this does not necessarily result in more damage between the boreholes. Damage depends on the distance between the boreholes, but also on the interaction of the stress waves. Damage creates heterogeneity in the medium, which affects propagation of stress waves produced by boreholes detonating later. Each hole, apart from damaging the material in its vicinity, preconditions material that is closer to the remaining holes, which upon their detonation result in increased levels of damage. This has been noted in fragmentation (Johansson and Ouchterlony 2013), where earlier detonated blasts precondition later detonating blasts, resulting in a reduction of the average fragment size. The results of the numerical model suggest that something similar occurs in delayed blasting where earlier detonating holes precondition the rock for the later detonating holes. However, the model of the calculations is continuum, so it cannot handle the effect that opened cracks would have on the stress wave propagation and, consequently, damage.

4 Discussion

From the previous observations, it is clear that the predictive tools to evaluate the effect of blasting on downstream operations are inaccurate. The effect on diggability was purposely left out, as the muckpile characteristics, which are affecting digging and are not clearly known. Productivity of crushers depends on the size distribution of the blasted rock. However, not even the 50% passing size of the fragmentation can be predicted accurately. Detailed geological information is not implemented in most predictive models. The effects of stress waves and timing are not explicitly described, explosive performance is only accounted based on total energy, and not in terms related to energy partition and scale is considered in a rudimentary way in Kuznetsov's equation.

Fragmentation distribution equations have parameters that need to be predicted accurately. For example, the uniformity index used in the popular Kuz–Ram model is calculated by Cunningham's equations (Cunningham 1983, 1987; 2005), which can be considered reasonable enough to provide trends as blasting parameters change. However, their accuracy may not be adequate as shown in Fig. 2, or claimed by Caceres et al. (2006).

Grindability changes due to blasting add to the complexity of the effect of blasting on size reduction. It is known that blasting modifies the grindability of rock. However, a relationship between blasting effort and grindability has been difficult to produce. Powder factor has been related to grindability in the small scale studies of our laboratory (Katsabanis and Kim 2011). Analysis and interpretation of the laboratory results in the previous sections suggest that high powder factors may be beneficial for grindability. Numerical modelling results suggest that to predict blast damage, which may be related to grindability, one needs to consider the distribution of powder, timing as well as the borehole pressures, which influence the stress waves and their interaction in a blast. Numerical modelling can provide some guidance on what is important; however, numerical models for stress wave propagation typically simplify reality. In the previous work, discontinuities and anisotropy were not considered in the simulations, while only stress wave propagation in a continuum was examined. However, despite the simplifications mentioned, the results are of value, since these numerical models accurately describe stress wave propagation in a fairly simple medium and enable the calculation of the resulting damage in the medium. Hence, they allow the performance of several numerical experiments, investigating the effect of blast design parameters in an ideal medium devoid of geologic complexities, thereby guiding further investigation and model formulation.

Developing an engineering model to predict grindability may be a challenge. Apart from the difficulties in calibrating a damage model and relating damage to grindability, the complex interaction of stress waves is probably impossible to be included in a comprehensive engineering model that predicts the effects of blasting on grinding. In addition, lithology is variable, even in the same blast, and needs to, somehow, be included. Ignoring lithology, even in the same blast as shown by some of the previous results (Table 2) confuse the analysis, thereby producing overwhelming amounts of scatter. Measurements, while drilling, promising in the modelling of fragmentation, may be useful to grindability as well.

While small-scale experiments and modelling are useful in identifying general trends, they seem to provide pertinent information only for the given lithology, blast geometry, explosive performance and delay time of the experiments or simulations.

Given the previous influences of a significant number of parameters, and the lack of detailed knowledge on the effect of each parameter on grindability, development of a predictive model needs large quantities of input data and a large number of observations. A possible way forward is through the analysis of industrial data that could provide many observations. For a data set to be of value, the following are needed:

- Information on lithology. Possible source are the measurements while drilling (MWD).
- Information on natural discontinuities. In this context, efforts using discrete fracture networks (DFN), providing information on the in situ block size distribution and the fracture intensity in the rock mass along with its variation, are promising (Junkin et al. 2019).
- Information on blasting. Blast geometry, timing, loading, explosive properties and local conditions.
- Blast fragmentation. The fragmentation of the material taken from the blast site and the exact location of the material prior to blasting must be known. Measurement of fragmentation is possible through image analysis, the accurate location of digging may be determined using the GPS location of the shovel and the displacement of the muckpile by the blast can be obtained through instrumentation, such as blast movement monitors (La Rosa et al. 2009)
- Crusher settings, throughput and energy use.
- Grinding settings, throughput and energy use.

The paramount point, in all the above, is the ability to follow the material from the bench or stope to the mill, so that blasting effort, result and lithology can be correlated. This is not a simple task as the material flows in ore passes, or is temporarily stocked in stockpiles. Cost efficient methods of tagging the material need to be developed for this purpose.

5 Conclusion

Blasting is the first stage of the comminution process and affects the results of subsequent operations. Fragmentation trends can be predicted reasonably well, but size prediction needs to be improved. The description of explosive performance and distribution need to be improved in the existing blast models. Delay time effects need to be extended beyond small-scale studies, and the assessment of blastability could utilize measurement while drilling (MWD) information. Increase in powder factor has led to increase in grindability in small-scale studies, but the effect is only quantified for small-scale experiments. It was shown that explosive performance in the hole, coupling medium, explosive charge distribution, delay time between boreholes, and blast geometry are important parameters affecting damage. To predict the effect of blasting on comminution, analysis of field data related to lithology, detailed blasting parameters and mill performance are needed.

Compliance with Ethical Standards

Conflict of interest The author declares that he has no conflict of interest.

References

Adebayo B, Bello WA (2014) Discontinuities effect on drilling condition and performance of selected rocks in Nigeria. Int J Min Sci Technol 24(5):603–608

Autodyn A (2009) Interactive non-linear dynamic analysis software, version 12, user's manual. SAS IP Inc., Canonburg

Bergmann OR, Wu FC, Edl JW (1974) Model rock blasting measures effect of delays and hole patterns on rock fragmentation: 8F, 1T, 20R. Engn. Min. J. V175, N6, June, 1974, P124–127. In: International journal of rock mechanics and mining sciences & geomechanics abstracts, vol 11, no. 11. Pergamon, p A233

Berry TF, Bruce RW (1966) A simple method of determining the grindability of ores. Can Min J 87:63–65

Blair DP (2010) Limitations of electronic delays for the control of blast vibration and fragmentation. In: Proceedings of the 9th international symposium on rock fragmentation by blasting, p 171

Brannon RM, Leelavanichkul S (2009) Survey of four damage models for concrete. Sandia Natl Lab 32(1):1–80

Caceres J, Katsabanis P, Pelley C, Kelebek S (2006) Maximizing NPV by Blasting. In: Conference proceedings. 8th international symposium on rock fragmentation by blasting, Santiago, Chile, pp 246–254

Cunningham C (1983) The Kuz–Ram Model for production of fragmentation from blasting. In: Proc. 1st Symp. on Rock Fragmentation by Blasting, Lulea

Cunningham CVB (1987) Fragmentation estimations and the Kuz–Ram model-four years on. In: Proc. 2nd int. symp. on rock fragmentation by blasting, pp 475–487

Cunningham CVB (2005) The Kuz–Ram fragmentation model-20 years on. In: Brighton conference proceedings, pp 201–210

Davis LL, Hill LG (2002) ANFO cylinder tests. In: AIP conference proceedings, vol 620, no. 1, pp 165–168

Dobratz BM, Crawford PC (1985) LLNL explosives handbook properties of chemical explosives and explosive simulants—LLNL University of California. Livermore, California–(UCRL–52997, 1985)

Esen S (2013) Fragmentation modelling and the effects of ROM fragmentation on comminution circuits. In: 23rd international mining congress & exhibition of Turkey, pp 252–260

Faramarzi F, Mansouri H, Farsangi ME (2013) A rock engineering systems based model to predict rock fragmentation by blasting. Int J Rock Mech Min Sci 60:82–94

Fried LE (1996) CHEETAH 1.39 user's manual. Lawrence Livermore National Laboratory, Livermore

Grundstrom C, Kanchibotla S, Jankovich A, Thornton D, Pacific DDNA (2001) Blast fragmentation for maximising the sag mill throughput at Porgera Gold Mine. In: Proceedings of the annual conference on explosives and blasting technique, vol 1, pp 383–400

Hikita DH (2008) The influence of blasting on Kemess hypogene ore milling. M.Sc. thesis. Queen's University at Kingston

Hudson JA, Harrison JP (2000) Engineering rock mechanics: an introduction to the principles. Elsevier, Oxford

Johansson D, Ouchterlony F (2013) Shock wave interactions in rock blasting: the use of short delays to improve fragmentation in model-scale. Rock Mech Rock Eng 46(1):1–18

Junkin WR, Ben-Awuah E, Fava L (2019) Incorporating DFN analysis in rock engineering systems blast fragmentation models. In: 53rd US rock mechanics/geomechanics symposium. American Rock Mechanics Association

Katsabanis PD, Gregersen S, Kunzel G, Pollanen M, Pelley C, Kelebek S (2005) Effects of blasting on damage and grindability of impacted rock. CIM Bull 1091:91

Katsabanis PD, Kim S (2011) Effect of blasting on impact breakage of the resulting fragments—results from small scale tests. Fragblast Int J Blast Fragment 5(2):87–108

Katsabanis PD, Omidi O (2015) The effect of the delay time on fragmentation distribution through small-and medium-scale testing and analysis. In: Proceedings of 11th international symposium on rock fragmentation by blasting (Fragblast 11), Sydney, Australia, pp 24–26

Katsabanis P, Omidi O, Rielo O, Ross P (2014) Examination of timing requirements for optimization of fragmentation using small scale grout samples. Blast Fragment 8(1):35–53

Katsabanis PD, Tawadrous A, Braun C, Kennedy C (2006) Timing effects on the fragmentation of small scale blocks of granodiorite. Fragblast 10(1–2):83–93

Kemeny JM, Kaunda RB, Streeter D, BoBo T (2003) Effect of blasting on the strength of rock fragments. In: Proceedings of the twenty-ninth conference on explosives and blasting technique, pp 381–390

Kim S (2010) An experimental investigation on the effect of blasting on impact breakage of rocks. M.Sc. thesis. Queen's University at Kingston

Khorzoughi MB, Hall R, Apel D (2018) Rock fracture density characterization using measurement while drilling (MWD) techniques. Int J Min Sci Technol 28(6):859–864

Kunzel G (2003) Study on blast damage development in small blocks and the effects on subsequent comminution. M.Sc. Thesis. Department of Applied Earth Sciences. TU Delft

La Rosa DM, Thornton DM, Wortley M (2009) U.S. Patent No. 7,490,507. Washington, DC: U.S. Patent and Trademark Office

Lilly PA (1986) An empirical method of assessing rock mass blastability. In: Proc. of large open pit mine conference, The Aus. Inst. of mining and metallurgy, pp 89–92

Latham JP, Lu P (1999) Development of an assessment system for the blastability of rock masses. Int J Rock Mech Min Sci 36(1):41–55

Michaux S, Djordjevic N (2005) Influence of explosive energy on the strength of the rock fragments and SAG mill throughput. Miner Eng 18(4):439–448

Morin MA, Ficarazzo F (2006) Monte Carlo simulation as a tool to predict blasting fragmentation based on the Kuz–Ram model. Comput Geosci 32(3):352–359

Napier-Munn et al (1996) Mineral comminution circuits. In: JKMRC monograph series in mining and mineral processing, JKMRC

Olsson M, Nie S, Bergqvist I, Ouchterlony F (2002) What causes cracks in rock blasting? Fragblast 6(2):221–233

Rai P, Schunnesson H, Lindqvist PA, Kumar U (2016) Measurement-while-drilling technique and its scope in design and prediction of rock blasting. Int J Min Sci Technol 26(4):711–719

Sanchidrián JA, Ouchterlony F (2017) A distribution-free description of fragmentation by blasting based on dimensional analysis. Rock Mech Rock Eng 50(4):781–806

Xie LX, Lu WB, Zhang QB, Jiang QH, Chen M, Zhao J (2017) Analysis of damage mechanisms and optimization of cut blasting design under high in-situ stresses. Tunn Undergr Sp Technol 66:19–33